

Brainstem activity, apnoea and death during seizures induced by intrahippocampal kainic acid in anaesthetised rats.

John G R Jefferys^{1,2}, Muhammad A Arafat^{1,3}, Pedro P Irazoqui^{1,3}, Thelma A Lovick^{1,4}

1. Weldon School of Biomedical Engineering, Purdue University, West Lafayette, IN, USA
2. Department of Pharmacology, Oxford University, Oxford, UK
3. Department of Electrical and Computer Engineering, Purdue University, West Lafayette, IN, USA
4. School of Physiology, Pharmacology and Neuroscience, University of Bristol, Bristol, UK

Corresponding authors: JGRJ and TAL

John G R Jefferys

Department of Pharmacology, University of Oxford, Mansfield Road, Oxford OX1 3QT, United Kingdom.

Phone +44 1865 556963

Fax +44 1865 271853

Email john.jefferys@pharm.ox.ac.uk

Orcid 0000-0003-0106-4412

Thelma A Lovick

School of Physiology, Pharmacology and Neuroscience, University of Bristol, Biomedical Sciences Building, University Walk, Bristol, BS8 1TD, United Kingdom

Phone +44 121 4271001

Email thelma.lovick@bristol.ac.uk

Orcid 0000-0002-7329-4607

Key words: heartrate, obstructive apnoea, status epilepticus, SUDEP

Running title: Seizures, brainstem and sudden death

17 text pages, 4401 words main text, 285 words summary/abstract, 0 tables, 6 main figures (1 colour), 3 supplementary figures (1 colour).

Abstract

Objective: To investigate how prolonged seizure activity impacts on cardiorespiratory function and activity of pre-Bötzinger complex, leading to sudden death.

Methods: Urethane-anaesthetized female Long-Evans rats were implanted with: nasal thermocouple, venous and arterial cannulae, and electrodes for ECG, hippocampal, cortical and brainstem recording. Kainic acid injection into the ventral hippocampus induced status epilepticus.

Results: Seizures caused hypertension, tachycardia and tachypnoea punctuated by recurrent transient apnoeas. Salivation increased considerably: in 11/12 rats, liquid with alkaline pH consistent with saliva was expelled from the mouth.

Most transient apnoeas were obstructive: nasal airflow ceased, while, in 83%, efforts to breathe persisted as continued rhythmic activity of respiratory pre-Bötzinger neurons, inspiratory EMG, and excursions of chest wall and abdomen. Blood pressure oscillated in time with respiratory efforts. This pattern also occurred in a minority of cases (16%) of incomplete apnoea, but not in rare cases (1%) of transient central apnoeas. During transient obstructive apnoeas the frequency of all inspiratory efforts decreased abruptly by ~30% suggesting a re-setting of the central respiratory rhythm generator.

22/31 rats died, due either to obstructive apnoea (12) or central apnoea following progressive slowing of respiration (10). Most rats dying of central apnoea had experienced several transient obstructive apnoeas.

Negative DC field potential shifts of the brainstem followed the final breath, consistent with previous reports on spreading depolarization in mouse models. Timing suggests the DC shift is a consequence rather than cause of respiratory collapse. Cardiac activity continued for tens of seconds.

Significance: Seizure activity in forebrain induces pronounced autonomic activation and disrupts activity in medullary respiratory centres, resulting in death from either obstructive or central apnoea. These results directly inform mechanisms of death in status epilepticus, and indirectly provide clues to mechanisms of SUDEP.

Introduction

Systemic epileptogenic agents directly access all parts of the brain, including those involved in cardiorespiratory control. Seizures are associated with significant autonomic and respiratory changes, which provide a potential cause of sudden unexpected death in epilepsy (SUDEP).¹ The MORTEMUS study² revealed 11 cases of SUDEP with cardiorespiratory monitoring. Respiration ceased within 11 minutes of a final generalised tonic-clonic seizure, following both cardiac and respiratory postictal abnormalities. This implicates respiratory failure as a major factor in sudden death.

Animal models are used to investigate how seizure activity may predispose to fatal cardiorespiratory events. Systemic kainic acid (KA) is commonly used to induce seizure activity in rodents, usually status epilepticus followed by repeated shorter-lasting seizures over several hours. Systemic KA produces sympathoactivation with pressor response, tachycardia and lengthening of QT interval.³⁻⁵ Respiration changes to shallow irregular breathing with gasping breaths interspersed with apnoeas, followed by sudden death due to laryngospasm in some animals.^{6; 7}

Two further hypotheses proposed to explain seizure-related apnoeas and fatal cardiorespiratory collapse are: (1) spreading depolarization (SD; similar to spreading depression) propagating from the forebrain into the brainstem, demonstrated in several mouse models;⁸⁻¹⁰ (2) laryngospasm triggered by gastric acid reflux; gastric acid reflux has been shown following systemic KA.¹¹

Although autonomic consequences of systemic KA have been attributed to the effects of seizure activity,⁵ and sympathetic and parasympathetic brainstem are activated during seizure activity,⁴ a contribution from KA acting directly on the brainstem cannot be excluded. Sympathoexcitatory glutamatergic actions at medullary sites are well established,¹² and direct application of KA to the ventral caudal medulla initially stimulates respiration followed by apnoea.¹³ The relative contribution to autonomic and respiratory changes of seizure activity versus direct effects of systemically-administered agents on brainstem control centres remains an open question, as does the fundamental question of whether seizure-related death is primarily caused by cardiac or respiratory malfunction.

To test the hypothesis that reported cardiorespiratory consequences, including deaths, of systemic KA^{6; 7; 11; 14} were due to seizures, rather than to its direct actions on brainstem sites, we induced seizures by local microinjection of KA directly into the hippocampus of

anaesthetised rats.¹⁵ Identical injections of dyes and other toxins show they are limited to the hippocampus.¹⁶ We recorded changes in cardiorespiratory variables that accompanied seizures, together with activity of respiratory-related neurons in the pre-Bötzinger complex, a key brainstem area for generating respiratory rhythm.^{17;18}

Status epilepticus evoked in acute preparations cannot, by definition, model SUDEP directly, but such models do present the opportunity for investigating fatal cardiorespiratory consequences associated with seizure activity. They are directly relevant to potential mechanisms of death in clinical status epilepticus, and may lead to hypotheses on SUDEP that should be tested in chronic models of self-limiting seizures.

MATERIALS AND METHODS

Experiments complied with Institutional Animal Care and Use Committee (IACUC) regulations, and used procedures approved by the Purdue Animal Care and Use Committee (PACUC). Rats lived under a 12:12 dark/light cycle, lights on at 0700, with free access to food and water until induction of anaesthesia.

Thirty-one female Long Evans rats (265-330 g; Envigo, Indianapolis, IN) were anaesthetised with urethane (1.4 g kg⁻¹ i.p.), a femoral artery was cannulated to measure blood pressure (BP), as was a femoral vein to administer saline (0.9%, 0.5 ml bolus i.v.) as required to maintain systolic pressure >100 mm Hg. We excluded 1/31 rats, because its baseline BP (102/54 mm Hg, mean 64 mm Hg) was much lower than the group mean (83.9±10.4 mm Hg) and failed to respond to saline injection. A thermostatically-controlled heating blanket maintained rectal temperature at 37°C (507223F, Harvard Apparatus, Cambridge, UK).

Urethane anaesthesia can lead to hyperglycaemia in fasted rats,¹⁹ but this effect is not significant in fed rats.²⁰ Therefore the proconvulsant effect of hyperglycaemia²¹ is not a confound in the present studies, which do not involve fasting. The oestrous cycle of the female rats could affect seizure susceptibility and increase variability in this study, however, oestrous cycle is reported not to affect duration or severity of status epilepticus induced by intrahippocampal KA.²²

The animal was mounted in a stereotaxic frame with the bregma-lambda axis horizontal. Measurements of nasal air temperature oscillations monitored respiration, using a thermocouple (5TC-TT-K-36-36, Omega, Egham, UK) in the nasal passage: in 12 rats

inserted through a small bur hole 7 mm rostral to the suture with the frontal bone, in 19 inserted into the nares. Rats are obligate nose-breathers, so that respiratory airflow can be detected by changes in temperature in the nasal passage²³ or outside the nares.²⁴ This inferred airflow parallels movements of the chest wall.²⁴ ECG was recorded by percutaneous needle electrodes inserted at right shoulder and left caudal thorax. In 11 rats the ECG contained a component of inspiratory EMG activity, extracted by thresholding low-amplitude troughs (~ 0.01 mV, c.f. ~ 1 mV ECG; Fig. 1). EMG-related events dominated sufficiently to make it unnecessary to remove ECG-related events (compare red and black events during first breath in Fig. 1). A respiration-related waveform was obtained using a Gaussian kernel.

Several bur holes were drilled in the skull for probes. A Hamilton microsyringe containing KA (10 mg.ml^{-1}) was positioned with its tip in right ventral hippocampus (5.4 mm caudal, 4.5 mm lateral to bregma, 6.8 mm below cortical surface); the target was CA3 stratum radiatum. ECoG was recorded from pairs of skull-screw electrodes inserted 2.5 mm caudal and 1.0 mm rostral to bregma, both 2.0 mm lateral of midline. In some rats we also recorded local field potential activity from ipsilateral dorsal hippocampus using bipolar 125- μm diameter platinum-iridium twisted-pair wire electrodes 3.6 mm caudal and 3.0 mm right of bregma, and 3.0 mm below cortical surface. Filters were 0.1-1000 Hz. Respiratory unit activity was recorded with 25- μm diameter parylene-insulated Pt/Ir wire, inserted using a system which rotates the electrode to allow it to penetrate the brain without bending.²⁵ The initial target in right brainstem pre-Bötzinger complex was 12.8 mm caudal and 0.6 mm left of bregma, for a 10° angle in the coronal plane to reach the target 1.9 mm right of bregma. If no respiratory-related neurons were found in the first track, the angle of subsequent tracks was varied up to 14° . Track length to recorded units was 6.7–7.8 mm below cerebellar surface. Recording bandwidth was 300-3500 Hz. In 5 experiments we also recorded DC to 3.5 kHz from the contralateral pre-Bötzinger region using a Teflon-coated 125- μm silver electrode conditioned by passing current for 6x1-minute periods (0.3 mA, normally requiring 2 V, sufficient for electrolysis), alternating direction to finish with the silver electrode negative. Reference electrode was placed in neighbouring scalp.

After preparation was complete, the brainstem recording electrode was advanced into the pre-Bötzinger complex until a neuron was isolated, with activity phase-locked to the nasal thermocouple signal. After ≥ 15 min baseline recording, 1-2 μl of KA was injected into the hippocampus over 5 min to induce seizure activity. Concern over the potency of our samples of KA led to use of higher doses, however dose had no significant effect on any of the

cardiorespiratory changes (Pearson correlation significance $p > 0.1$ for each). Time between induction of anaesthesia and injection of KA. Time between induction of anaesthesia and injection of KA averaged 295 ± 107 min, the main source of variation being time required to find units.

Data were captured using Neurolog (Digitimer, Welwyn, UK), Grass (Grass Instrument Co, Quincy MA) and custom-made amplifiers, and a Power 1401 signal acquisition unit with Spike2 software (Cambridge Electronic Design, Cambridge, UK). Analysis was performed in Spike2. Off-line signal conditioning included: the “HumRemove” script to remove mains-related noise (particularly for brainstem units), smoothing (50 ms time-constant for nasal temperature signals), the peak detection feature of Spike2 provided heartrate from the BP signal and respiratory rate from the nasal temperature signal.

Statistical analyses used SPSS version 23 (IBM, New York). Results are expressed as mean \pm SD unless otherwise stated. Data were tested for normality, and non-parametric tests used where appropriate.

RESULTS

Cardiorespiratory changes during seizure activity

Following intrahippocampal KA, spontaneous electrographic activity attenuates and is replaced by seizure activity (rhythmic synchronous field potentials in hippocampal and/or cortical recording electrodes; Fig. 2). Seizure activity develops in all animals, starting 1.5-8 min after the start of the injection, and is associated with pronounced cardiorespiratory changes characterised, in all but one animal, by hypertension, tachycardia and hyperpnoea (Fig. 2). Mean arterial pressure increases from 83.9 ± 10.4 to 138.3 ± 19.6 mm Hg (paired t-test; $p < 0.001$), heartrate rises from 342.1 ± 48.5 to 486.8 ± 38.2 beats min^{-1} (paired t-test; $p < 0.001$), respiratory rate more than doubles from 97.5 ± 30.0 to 226.0 ± 91.2 breaths min^{-1} (related-samples Wilcoxon Signed Rank Test; $p < 0.001$). Time course of cardiorespiratory responses varies between rats, but all follow a similar pattern. Time from start of injection until onset is: BP 204.9 ± 149.1 s, heartrate 500.3 ± 324.1 s, and respiratory rate 402.8 ± 301.2 s. Most rats develop a prominent, usually bilateral, exophthalmos, and rapid vibrissal movements. Other motor signs of seizures observed when KA is administered to conscious rats, are absent.

Augmented breaths

Augmented breaths (sighs) comprise prolonged inspiration and increased tidal volume followed by a respiratory pause and several seconds of faster breathing (Fig. 3).²⁶

For quantification, we define an augmented breath as an excursion of the nasal air temperature signal $\geq 2\times$ baseline amplitude. Before KA injection augmented breaths are infrequent: 30% of rats make none; incidence in the remainder is $0.34 \pm 0.21 \text{ min}^{-1}$. In all but one of the rats in this latter group, augmented breaths cease for $10.2 \pm 8.4 \text{ min}$ following KA injection, before resuming at a significantly higher rate ($2.2 \pm 1.2 \text{ min}^{-1}$; $p < 0.001$, paired t-test). In the rats without augmented breaths before KA injection, they appear in all but one rat between 6 and 65 min (median 17) after the injection start, continuing at $1.81 \pm 1.5 \text{ min}^{-1}$. As tachypnoea strengthens with seizure progression, the number of augmented breaths increases substantially as a fraction of all breaths (Fig. 3).

Transient apnoeas.

The most common respiratory disturbances are transient apnoeas, which developed in all but two rats. Transient apnoeas are characterised by abrupt cessation of nasal air temperature oscillations, followed a variable time later by an abrupt resumption (Fig. 4). We use 5-s as a minimum duration for measuring apnoeas; shorter apnoeic periods also occur, sometimes in clusters. If no or few apnoeas develop by 2 h after intrahippocampal KA (in 2 rats), we give a second injection to promote apnoeas. Peak cardiorespiratory changes occurred before the second injection in both cases. The latency to first apnoea from the start of the preceding (or only) KA injection is 4-149 min, mean $63.3 \pm 44.4 \text{ min}$. The one rat with no apnoeas until the second injection has a latency of 125 min from the first injection, and increases the mean latency to $69.0 \pm 44.2 \text{ min}$. We analyse 267 apnoeas from 23 rats. The number analysed varies considerably between rats (2-39 per rat, 11.4 ± 10.8); duration of each ranges between 5-15 s ($10.6 \pm 7.1 \text{ s}$).

Obstructive apnoeas.

Despite inter-animal variability in frequency and timing, the majority of transient apnoeas displayed features consistent with airway obstruction (Fig. 4A).

Activity of neurons in the pre-Bötzinger region. Pre-Bötzinger neurons show ongoing phasic activity time-locked to nasal temperature oscillations. Firing typically precedes onset of inspiration (decrease in nasal air temperature) by 140-170 ms (Fig. 4). In some cases of low signal/noise ratio we measure root-mean-square amplitude of the brainstem recording to

detect multi-unit activity. We record phasic respiratory-related units from the pre-Bötzinger region during 61 apnoeas in 8 rats. When nasal airflow ceases, the units continue to fire rhythmically but at a significantly lower frequency than for eupnoea. Burst rate during apnoeas decreases from 119.3 ± 25.1 to $73.6 \pm 18.4 \text{ min}^{-1}$, $p < 0.0005$, paired t-test), a $37.8 \pm 10.2\%$ reduction in frequency of oscillations of the Bötzinger respiratory rhythm generator. In 14 apnoeas lasting $>10\text{s}$ ($14.7 \pm 3.75 \text{ s}$) the frequency of oscillations in unit firing during the first 5s and last 5s do not differ significantly ($71.0 \pm 11.8 \text{ min}^{-1}$ vs. $68.3 \pm 15.2 \text{ min}^{-1}$; $p > 0.05$, paired t-test) suggesting that the network oscillator switches to a new state at the onset of apnoea rather than slowing down gradually as the rat struggled ineffectively to breath. Once breathing re-starts, unit firing returns abruptly to the rate time-locked to the nasal signal.

Respiratory effort during apnoeas. Visual observation during periods of arrested nasal airflow clearly showed the rats continued to make respiratory effort, evidenced by movements of the thorax and abdomen. In 11 rats the signal recorded from the chest leads contained in addition to ECG, an EMG component time-locked to the inspiratory phase of the nasal air temperature signal (Fig. 1; Fig. 4A). By extracting this component, we monitor inspiratory EMG activity during apnoeas. In cases of simultaneous recording of EMG and pre-Bötzinger unit activity, their frequencies correspond closely. As with unit activity, respiratory EMG continued at a significantly lower frequency during arrested nasal airflow. Recordings of 94 apnoeas reveal the frequency of inspiratory EMG activity decreases from 124.4 ± 44.8 to $75.9 \pm 21.9 \text{ min}^{-1}$; $p < 0.0005$, paired t-test, confirming continued but slower respiratory effort when nasal airflow had ceased.

BP and heartrate. During apnoeas BP become unstable and oscillations develop at the same frequency as the continuing inspiratory effort, likely reflecting changes in venous return due to large fluctuations in intrathoracic pressure as the rat strived, ineffectively, to breath. These observations are consistent with cessation of nasal air flow due to airway obstruction.

A minority of transient apnoeas share features with obstructive apnoeas outlined above, but with an abrupt, $>50\%$ reduction in amplitude, rather than complete cessation, of the nasal airflow signal (42 episodes in 3 rats and one each in two others). These partial apnoeas last 5-12 s ($7.1 \pm 2.9 \text{ s}$). Like the complete apnoeas described above, onset and offset are abrupt and unpredictable. Although effective respiration continued, the frequency of the nasal temperature signal reduces from $186.4 \pm 64.1 \text{ min}^{-1}$ to $100.6 \pm 33.9 \text{ min}^{-1}$. Oscillations in the BP

signal are at the same frequency as respiration. One rat with simultaneous recordings of both pre-Bötzinger region units and inspiratory muscle EMG extracted from the ECG signal, the frequency of both decreases in line with the nasal airflow signal.

Central apnoeas

Four transient apnoeas from 3 rats lack evidence of continued respiratory effort during cessation of nasal air flow (Fig. 4C, lasting 21.0 ± 9.9 s), suggesting failure of central respiratory drive mechanisms. In these cases, rhythmic EMG and BP oscillations cease during the apnoea. With continuing apnoea, heartrate slows by 144.5 ± 102.9 beats min^{-1} and BP falls by 20.1 ± 11.4 mm Hg. On 3 occasions obstructive apnoeas precede a central apnoea, separated by a single breath (Fig. S2).

Oral secretions.

In several early experiments we noted an accumulation of liquid in the mouth towards the end of the experiment. In 12 rats we collect overflowing liquid, which was found in 11 (weight 30-300 μg). The liquid proved to be alkaline (pH 9), consistent with rat saliva.²⁷

Spontaneous deaths

Twenty-two rats die spontaneously after injecting KA. We terminate the experiment if either the time under anaesthesia exceeds 7.5 hours or 4 hours elapses after KA injection (8 rats). Twelve rats die of obstructive apnoea, 119.5 ± 46.0 min after injection of KA (Fig. 5A, Fig. 6A, Fig. S1B). The onset of terminal apnoea does not appear to differ from the preceding transient apnoeas (3-39). After nasal airflow flow ceases, respiratory effort (from brainstem activity, EMG and/or visual observation) continues for ≤ 43 s before BP and heartrate begin a sharp terminal decline. Median delay from last breath to the start of the rapid drop in heartrate is 15 s, (interquartile range 9-18 s; Fig. S1). Active inspiratory efforts in the absence of nasal airflow suggest that the cause of death is obstructive apnoea. In 11/12 rats recording of pre-Bötzinger neuronal activity continues through the final apnoea. In 9 an intense desynchronised electrical discharge begins 17.9 ± 8.6 s from the cessation of nasal airflow, increasing from 15 to 150 Hz (median increase 140 Hz, interquartile range 56-243 Hz; Fig. 5A, Fig. S1).

The remaining 10 lethal apnoeas are not obstructive: evidence of respiratory drive stops at the last breath (from pre-Bötzinger activity in 4 cases, BP oscillations in 8, and/or EMG in 8), suggesting a central mechanism. In 3/10 rats the primary response to intrahippocampal KA is

progressive slowing of respiration culminating in death within 34 min. In the remaining 7, intrahippocampal KA initially produces tachypnoea punctuated with obstructive apnoeas. Then 2-13 min after respiratory rate returns to baseline, respiration slows progressively until the rat dies, a total of 48.0 ± 33.2 min after KA injection, excluding one outlier of 225 min (Fig. 5B, Fig. 6B). These rats lack the large desynchronised electrical hyperactivity of the brainstem associated with lethal obstructive apnoeas (median firing increase 0 Hz, interquartile range -6 to 0 Hz Fig. 6B, Fig. S1A). Cardiorespiratory responses to KA do not differ between rats dying from central or obstructive apnoea, with the exception that central cases started with faster baseline heartrate than obstructive cases (356 ± 26 vs 313 ± 43 bpm; t-test $p < 0.05$; Supplemental Fig. S3).

Cardiac function during terminal apnoea.

BP and heartrate deteriorate following the collapse of respiration. Heartrate decreases rapidly 10-20s after the last breath (Fig. 5, Fig. 6, Fig. S1C-E). Obstructive and central terminal apnoeas do not differ in extent, latency or duration of the rapid decrease in heartrate (Fig. S1C-E). They only differ in the late brainstem discharge and in the nature of the lethal apnoea.

Brainstem DC changes.

DC pre-Bötzinger recordings in 5 rats reveal no consistent changes in DC signal during transient apnoeic periods. Prolonged negative DC shifts are linked to spreading depolarisation. We assess the temporal relationship of DC shifts in pre-Bötzinger potential, defined by time course slower than 20s, with respiratory arrest and ECG changes. In all cases a terminal DC shift of -2.5 ± 1.2 mV follows the final effective breath after 16.5 ± 13.3 s, whether obstructive or central (Fig. 6 A, B). In the case of obstructive apnoeas, a burst of neuronal firing precedes the negative shift. The relationship of the rapid decrease of heartrate with brainstem bursts and DC shifts is more variable. In 2/5 cases (1 obstructive, 1 central) the heartrate drop precedes pre-Bötzinger DC shifts; in the remaining 3/5 (2 obstructive, 1 central), the heartrate drop follows DC shifts.

DISCUSSION

Status epilepticus evoked by intrahippocampal KA causes pronounced changes in cardiorespiratory function. As seizures develop, BP, heartrate and respiration rate increase substantially. Tachypnoea is interrupted periodically by transient apnoeas. Of 22 rats that die

following KA injection, 12 (55%) die from obstructive apnoea, failing to breath despite continuing, ineffective, centrally-driven respiratory efforts. In the remaining rats, death also results from respiratory failure but without evidence of efforts to breath; 3 die following progressive slowing of respiration after KA injection, 7 experience tachypnoea before progressive slowing and death.

Cardiovascular changes.

The tachycardia and hypertension following intrahippocampal KA resembles previous reports on systemic convulsants in anaesthetised rats and cats, which implicate pronounced sympathactivation alongside near-maximal increases in parasympathetic activity.^{4; 6; 28; 29} Others report bradycardia with arrhythmia.^{4; 30} This discrepancy could depend on relative levels sympathetic and parasympathetic activity and/or on starting heartrate.³¹ Other confounds include: strain differences in susceptibility,³² sex, type of anaesthetic, convulsant and route of administration. Unlike focal injections into a restricted area of the brain, systemic administration of convulsants may include widespread non-seizure-related responses to actions at multiple cardiorespiratory centres.

Respiration.

KA injection into ventral hippocampus causes a substantial increase in respiratory rate, consistent with previous findings from SE induced acutely by systemic agents in anaesthetised rats, cats and piglets.^{6; 7; 29; 33} In contrast, slowing of respiration is reported following focal ventral hippocampal microinjection of another excitatory amino acid (DLH).³⁴ However, that effect is short-lasting (<20min) and selective for CA1 pyramidal layer. Time-limited (1-2 min) seizures induced by brief (2-s) electrical stimulation of dorsal hippocampus also slow respiration, attributed to alterations in serotonergic neuron activity in the raphe nuclei.³⁰ The contrast with the substantial long-lasting increase in respiratory rate we find likely is due to the prolonged seizures induced by larger-volume injections of KA. Urethane anaesthesia raises basal respiratory rate in both mice³⁵ and rats.³⁶ We report that status and recurrent seizures substantially increase respiration rate from the baseline established under urethane. It is conceivable that the cumulative effects of urethane and seizures drives tachypnoea to levels that trigger fatal apnoeas, however deaths occur after the tachypnoea passed its peak, so we conclude that this is unlikely. As with all acute experiments under anaesthesia we need to remember that anaesthetics affect brain and

systemic physiology, and that conclusions ultimately need to be tested in unanaesthetised preparations.

Microinjection of DLH into CA1 suppresses augmented breaths for several minutes,²⁶ as we report here for KA. However, the DLH study does not report the subsequent long-lasting increase in frequency of augmented breaths found in our experiments. Differences most likely result from different patterns of activity imposed on brainstem respiratory centres by seizure- and non-seizure-associated activation of the ventral hippocampus.

Transient apnoeas.

Prolonged seizures induced by KA, both intrahippocampal and systemic,⁶ lead to transient apnoeas of similar duration and appearance. Their incidence is considerably greater following intrahippocampal administration, and almost all are obstructive: airflow ceases, brainstem respiratory neurons continue firing rhythmically, matched by respiratory muscle activity and intrathoracic pressure oscillations large enough to modulate BP. In marked contrast, transient apnoeas following systemic KA occur with an open glottis, leaving failure of central respiratory drive as the only plausible mechanism.⁶ The reason for this difference is unclear; we can exclude differences in rat strain and sex, and in recording methods because we also find transient central apnoeas when we inject KA systemically (R.B.Budde, D.J.Pederson, E.N.Biggs, J.G.R.Jefferys, P.P.Irazoqui, submitted). Four transient apnoeas following intrahippocampal KA (in 3 rats) are central (Fig. 4C): rhythmic activity ceases of both respiratory units and respiratory muscles, and BP oscillations fail to appear. They cause transient progressive bradycardia and decline in BP.

During transient obstructive apnoeas, the pre-Bötzinger respiratory rhythm resets to a lower frequency. This effect is not secondary to occlusion of the airway since a similar slowing of respiration occurs during partial apnoeas, with reduced rather than absent airflow. The lower frequency remains constant during each apnoea, suggesting a state change in the respiratory rhythm generator that coincides with the cessation of effective respiration. This could be a feature of local networks in the pre- Bötzinger complex; alternatively, control of frequency could switch to other parts of the wider brainstem respiratory rhythm generator.³⁷ A key question is how obstruction of the airway is associated with respiratory rhythm. Laryngeal motor neurons are located in nucleus ambiguus³⁸ and receive direct inputs from hippocampus.³⁹ During apnoeas the abnormal activity from the forebrain could activate

laryngeal pre-motor neurons in parallel with switching the respiratory rhythm network to a lower frequency.

Lethal apnoeas.

The majority of rats in our study die from a lethal apnoea after prolonged seizures. Most apnoeas are obstructive, on the basis of continuation of respiratory effort, but a substantial minority are central. Systemic KA also leads to lethal apnoeas,^{6; 7; 11} but always obstructive, and associated with laryngospasm resulting from increased descending activity in the recurrent laryngeal nerve.

Hypotheses for lethal apnoeas

Gastric acid reflux. Previously we reported that systemic administration of KA caused gastric acid reflux, which could provoke laryngospasm.¹³ However, KA application to brainstem structures⁴⁰ is reported to stimulate production of gastric acid, raising the possibility that this effect is independent of seizures. The salivation we report here does not support gastric acid reflux, but cannot exclude the mechanism. The rapid onset and termination of the brief transient obstructive apnoeas also are hard to reconcile with laryngospasm triggered by oesophageal acid.

Brainstem spreading depolarization (SD) is proposed as a mechanism for cardiorespiratory failure. Mice with two epilepsy-related genetic modifications develop brainstem SD following induced seizures,⁸ as does a familial hemiplegic migraine mutation.¹⁰ Another mutation, associated with sudden cardiac death and SUDEP,⁹ reduces SD threshold in both neocortex and brainstem. Our DC recordings from the brainstem of wild-type rats show the DC shift in pre-Bötzinger always follows the cessation of airflow at the onset of terminal apnoea, whether obstructive or central, which is inconsistent with SD causing apnoea. Precise timing is crucial, and needs to relate airflow (not only respiratory effort) to SD or other neural pathophysiology. Anaesthesia in mice delays the lethal apnoea and SD,¹⁰ but does not change the threshold, amplitude and propagation rate of cortical spreading depression,⁴¹ from which we conclude that while the timing of apnoea and spreading depolarisation may be slowed by anaesthesia, the fundamental pathophysiology is likely preserved.

Obstructive terminal apnoeas are associated with brainstem hyperactivity that could be consistent with the onset of SD. The absence of this hyperactivity from terminal central apnoeas shows it is not required for SD. In both cases the most likely cause of DC shifts in extracellular fields is K^+ efflux resulting from hypoxia once respiration has ceased. The

timing of cardiac decline is less clear. Terminal cardiac decline/collapse always follows respiratory arrest, but the most rapid decrease in heart rate can either precede or follow the onset of the DC shift in pre-Bötzinger. We cannot exclude SD or a similar event originating in dorsal medullary cardiovascular control centres contributing to cardiac failure:⁸ the slow propagation velocity of SD requires additional DC recordings in cardiovascular brainstem structures to address that question. However, it also is possible that DC shift and cardiac run-down are united by dependence on hypoxia.

In seeking alternative mechanisms for lethal apnoeas we need to consider obstructive and central apnoeas separately. Obstructive apnoeas are likely due to closure of the larynx, potentially due to hyperactivity of laryngeal motor neurons in nucleus ambiguus,⁴² perhaps driven by descending drive from seizing forebrain structures. In contrast, central apnoeas may be due to suppression of the brainstem, possibly analogous to post-ictal EEG suppression. The absence of brainstem hyperactivity preceding SD following central terminal apnoeas is consistent with reduced excitability.

Conclusions

Prolonged seizure activity induces dramatic cardiorespiratory disturbances, which can lead to sudden death due to failure of respiration. Deaths during acute SE in animal models under anaesthesia is a model of death from status rather than from SUDEP. However, they do open a window on how seizure activity impacts on the respiratory control network. The choice of model is important. Whilst both systemic and focal administration of epileptogenic agents produce the same lethal consequences, cessation of respiration, the underlying mechanisms differ. In particular, direct actions of the stimulant on brainstem control centres may be a confound during seizure activity evoked by systemic administration of epileptogenic agents. Nevertheless, all studies point to apnoea as a likely cause of death in SUDEP³¹ and highlight the need for further studies in chronic epilepsy models.

Ethical publication

We confirm that we have read the Journal's position on issues involved in ethical publication and affirm that this report is consistent with those guidelines.

Conflicts of Interest

Authors declare that they have no conflicts of interest.

1. Devinsky O, Hesdorffer DC, Thurman DJ, et al. Sudden unexpected death in epilepsy: epidemiology, mechanisms, and prevention. *Lancet Neurol* 2016;15:1075-1088; Dlouhy BJ, Gehlbach BK, Richerson GB. Sudden unexpected death in epilepsy: basic mechanisms and clinical implications for prevention. *J Neurol Neurosurg Psychiatry* 2016;87:402-413.
2. Ryvlin P, Nashef L, Lhatoo SD, et al. Incidence and mechanisms of cardiorespiratory arrests in epilepsy monitoring units (MORTEMUS): a retrospective study. *Lancet Neurol* 2013;12:966-977.
3. Hotta H, Koizumi K, Stewart M. Cardiac sympathetic nerve activity during kainic acid-induced limbic cortical seizures in rats. *Epilepsia* 2009;50:923-927.
4. Sakamoto K, Saito T, Orman R, et al. Autonomic consequences of kainic acid-induced limbic cortical seizures in rats: peripheral autonomic nerve activity, acute cardiovascular changes, and death. *Epilepsia* 2008;49:982-996.
5. Bhandare AM, Kapoor K, Pilowsky PM, et al. Seizure-Induced Sympathoexcitation Is Caused by Activation of Glutamatergic Receptors in RVLM That Also Causes Proarrhythmogenic Changes Mediated by PACAP and Microglia in Rats. *J Neurosci* 2016;36:506-517.
6. Nakase K, Kollmar R, Lazar J, et al. Laryngospasm, central and obstructive apnea during seizures: Defining pathophysiology for sudden death in a rat model. *Epilepsy Res* 2016;128:126-139.
7. Villiere SM, Nakase K, Kollmar R, et al. Seizure-associated central apnea in a rat model: Evidence for resetting the respiratory rhythm and activation of the diving reflex. *Neurobiol Dis* 2017;101:8-15.
8. Aiba I, Noebels JL. Spreading depolarization in the brainstem mediates sudden cardiorespiratory arrest in mouse SUDEP models. *Sci Transl Med* 2015;7:282ra246.
9. Aiba I, Wehrens XH, Noebels JL. Leaky RyR2 channels unleash a brainstem spreading depolarization mechanism of sudden cardiac death. *Proc Natl Acad Sci U S A* 2016;113:E4895-4903.
10. Loonen ICM, Jansen NA, Cain SM, et al. Brainstem spreading depolarization and cortical dynamics during fatal seizures in Cacna1a S218L mice. *Brain* 2019;142:412-425.
11. Budde RB, Arafat MA, Pederson DJ, et al. Acid reflux induced laryngospasm as a potential mechanism of sudden death in epilepsy. *Epilepsy Res* 2018;148:23-31.
12. Dampney RA, Horiuchi J, Tagawa T, et al. Medullary and supramedullary mechanisms regulating sympathetic vasomotor tone. *Acta Physiol Scand* 2003;177:209-218.
13. Martin RL, Sinclair JD. Kainic acid on the rat ventral medullary surface depresses hypoxic and hypercapnic ventilatory responses. *Respir Physiol* 1990;80:55-70.
14. Stewart M, Kollmar R, Nakase K, et al. Obstructive apnea due to laryngospasm links ictal to postictal events in SUDEP cases and offers practical biomarkers for review of past cases and prevention of new ones. *Epilepsia* 2017.
15. Bragin A, Engel J, Jr., Wilson CL, et al. Electrophysiologic analysis of a chronic seizure model after unilateral hippocampal KA injection. *Epilepsia* 1999;40:1210-1211.
16. Ferecsko AS, Jiruska P, Foss L, et al. Structural and functional substrates of tetanus toxin in an animal model of temporal lobe epilepsy. *Brain Struct Funct* 2015;220:1013-1029.
17. Munoz-Ortiz J, Munoz-Ortiz E, Lopez-Meraz ML, et al. Pre-Botzinger complex: Generation and modulation of respiratory rhythm. *Neurologia* 2016;doi 10.1016/j.nrl.2016.05.011.
18. Ikeda K, Kawakami K, Onimaru H, et al. The respiratory control mechanisms in the brainstem and spinal cord: integrative views of the neuroanatomy and neurophysiology. *J Physiol Sci* 2017;67:45-62.

19. Wang MY, Ren LM, Du ZJ, et al. Urethane-induced hyperglycemia. *Acta Pharmacol Sin* 2000;21:271-275.
20. Sánchez-Pozo A, Alados JC, Sánchez-Medina F. Metabolic changes induced by urethane-anesthesia in rats. *Gen Pharmacol* 1988;19:281-284.
21. Huang CW, Cheng JT, Tsai JJ, et al. Diabetic hyperglycemia aggravates seizures and status epilepticus-induced hippocampal damage. *Neurotox Res* 2009;15:71-81.
22. Rattka M, Brandt C, Loscher W. The intrahippocampal kainate model of temporal lobe epilepsy revisited: epileptogenesis, behavioral and cognitive alterations, pharmacological response, and hippocampal damage in epileptic rats. *Epilepsy Res* 2013;103:135-152.
23. Ranade S, Hangya B, Kepecs A. Multiple modes of phase locking between sniffing and whisking during active exploration. *J Neurosci* 2013;33:8250-8256.
24. Wilson DA, Sullivan RM. Respiratory airflow pattern at the rat's snout and an hypothesis regarding its role in olfaction. *Physiol Behav* 1999;66:41-44.
25. Arafat MA, Rubin LN, Jefferys JGR, et al. A method of flexible micro-wire Electrode insertion in rodent for chronic Neural Recording and a device for electrode insertion. *IEEE Trans Neural Syst Rehabil Eng* 2019.
26. Ajayi IE, Mills PC. Effects of the hippocampus on the motor expression of augmented breaths. *PLoS One* 2017;12:e0183619.
27. Djekoun-Bensoltane S, Kammerer M, Larhantec M, et al. Nitrate and nitrite concentrations in rabbit saliva Comparison with rat saliva. *Environ Toxicol Pharmacol* 2007;23:132-134.
28. Bhandare AM, Mohammed S, Pilowsky PM, et al. Antagonism of PACAP or microglia function worsens the cardiovascular consequences of kainic-acid-induced seizures in rats. *J Neurosci* 2015;35:2191-2199.
29. Paydarfar D, Eldridge FL, Wagner PG, et al. Neural respiratory responses to cortically induced seizures in cats. *Respir Physiol* 1992;89:225-237.
30. Zhan Q, Buchanan GF, Motelow JE, et al. Impaired serotonergic brainstem function during and after seizures. *J Neurosci* 2016;36:2711-2722.
31. Stewart M. An explanation for sudden death in epilepsy (SUDEP). *J Physiol Sci* 2018;68:307-320.
32. Bertoglio D, Amhaoul H, Van Eetveldt A, et al. Kainic acid-induced post-status epilepticus models of temporal lobe epilepsy with diverging seizure phenotype and neuropathology. *Front Neurol* 2017;8:588.
33. Terndrup TE, Darnall R, Knuth SL, et al. Effects of experimental cortical seizures on respiratory motor nerve activities in piglets. *J Appl Physiol* 1999;86:2052-2058.
34. Ajayi IE, McGovern AE, Driessen AK, et al. Hippocampal modulation of cardiorespiratory function. *Respir Physiol Neurobiol* 2018;252-253:18-27.
35. Massey CA, Richerson GB. Isoflurane, ketamine-xylazine, and urethane markedly alter breathing even at subtherapeutic doses. *J Neurophysiol* 2017;118:2389-2401.
36. Silva NF, Pires JG, Campos RR, et al. Cardiovascular and respiratory responses to microinjection of L-glutamate into the caudal pressor area in conscious and anesthetized rats. *Braz J Med Biol Res* 2001;34:1603-1606.
37. Anderson TM, Ramirez JM. Respiratory rhythm generation: triple oscillator hypothesis. *F1000Res* 2017;6:139.
38. Lobera B, Pasaro R, Gonzalez-Baron S, et al. A morphological study of ambiguous nucleus motoneurons innervating the laryngeal muscles in the rat and cat. *Neurosci Lett* 1981;23:125-130.
39. Van Daele DJ, Cassell MD. Multiple forebrain systems converge on motor neurons innervating the thyroarytenoid muscle. *Neurosci* 2009;162:501-524.

40. White RL, Jr., Rossiter CD, Hornby PJ, et al. Excitation of neurons in the medullary raphe increases gastric acid and pepsin production in cats. *Am J Physiol* 1991;260:G91-96; Yang H, Yuan PQ, Wang L, et al. Activation of the parapyramidal region in the ventral medulla stimulates gastric acid secretion through vagal pathways in rats. *Neurosci* 2000;95:773-779.
41. Houben T, Loonen IC, Baca SM, et al. Optogenetic induction of cortical spreading depression in anesthetized and freely behaving mice. *J Cereb Blood Flow Metab* 2017;37:1641-1655.
42. Weissbrod P, Pitman MJ, Sharma S, et al. Quantity and three-dimensional position of the recurrent and superior laryngeal nerve lower motor neurons in a rat model. *Ann Otol Rhinol Laryngol* 2011;120:761-768.

Supplemental Material

Supplemental Fig. S1

Brainstem discharge and heartrate collapse following final breath. **A.** Increased maximal brainstem firing rate 10-20 s after final breath or attempt to breath as a multiple of maximal firing rate during the previous 10 s (change: $p < 0.001$ Mann-Whitney U test). Firing rate is measured by rate of crossings of a threshold voltage. **B.** Obstructive fatal apnoea showing continued rhythmic activity of brainstem respiratory neurons after final breath, followed by large neuronal discharge (shown on r.m.s., raw signal and firing rate). ECG shows visible slowing, quantified in the heartrate trace below. The remainder of this figure concerns the most abrupt section of the heartrate drop, which is clearly visible in the raw ECG trace. **C.** The rapid drop in heartrate does not differ significantly between rats dying from obstructive (red lines) and central (dashed blue lines) apnoeas. Each line represents one rat ($p = 0.014$; HR before drop is significantly lower for central apnoeas, $p \leq 0.003$, but HR after is not, $p = 0.14$). **D.** Latency to onset of rapid HR drop does not differ between obstructive and central terminal apnoeas ($p = 0.18$, Mann-Whitney U test). **E.** Duration of rapid HR drop does not differ between obstructive and central apnoeas. Statistics are cited in the main text ($p = 0.70$, Mann-Whitney U test).

Supplemental Fig. S2

Sequential obstructive and central transient apnoeas. Prolonged (26-s) apnoea split by a single breath with a preceding obstructive apnoea lasting 15 s and a subsequent central apnoea lasting 10.5 s. Respiratory brainstem activity is visible during the obstructive apnoea but not during the central apnoea. Blood pressure oscillates with attempts to breath during obstructive apnoea, but declines smoothly during central apnoea, and also at the very start of the whole event.

Supplemental Fig. S3

Physiological changes preceding deaths by apnoea that are obstructive (boxes labelled “o”) and central (“c”). Seizure-related increases in BP (Δ BP) and respiration rate (Δ RR) did not differ between the two groups (t tests $P = 0.32$ and 0.8 , respectively), but heartrate did (Δ HR; t-test $P < 0.005$). All 3 physiological measures approach their maximal values during seizures, including heartrate, so maximal heartrate did not differ between the two groups ($P = 0.12$) but the baseline heartrate preceding KA injection did ($P < 0.04$). The relevance, and robustness, of this observation remains to be determined.

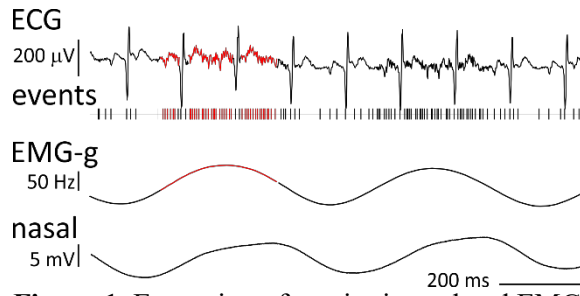


Figure 1. Extraction of respiration-related EMG from ECG recording. ECG in lead 2 configuration includes low-amplitude activity superimposed on the normal components of the ECG (marked in red for first breath). Events mark low-threshold troughs detected in SPIKE2, and include both low-amplitude signals (red, for first breath) and high-amplitude ECG. Applying Gaussian kernel with time constant 250 ms produces a waveform “EMG-g”, with no phase lag, that is locked to the signal from the nasal thermocouple. Red colour follows the putative respiratory EMG of the first breath from raw ECG to smoothed EMG-related waveform.

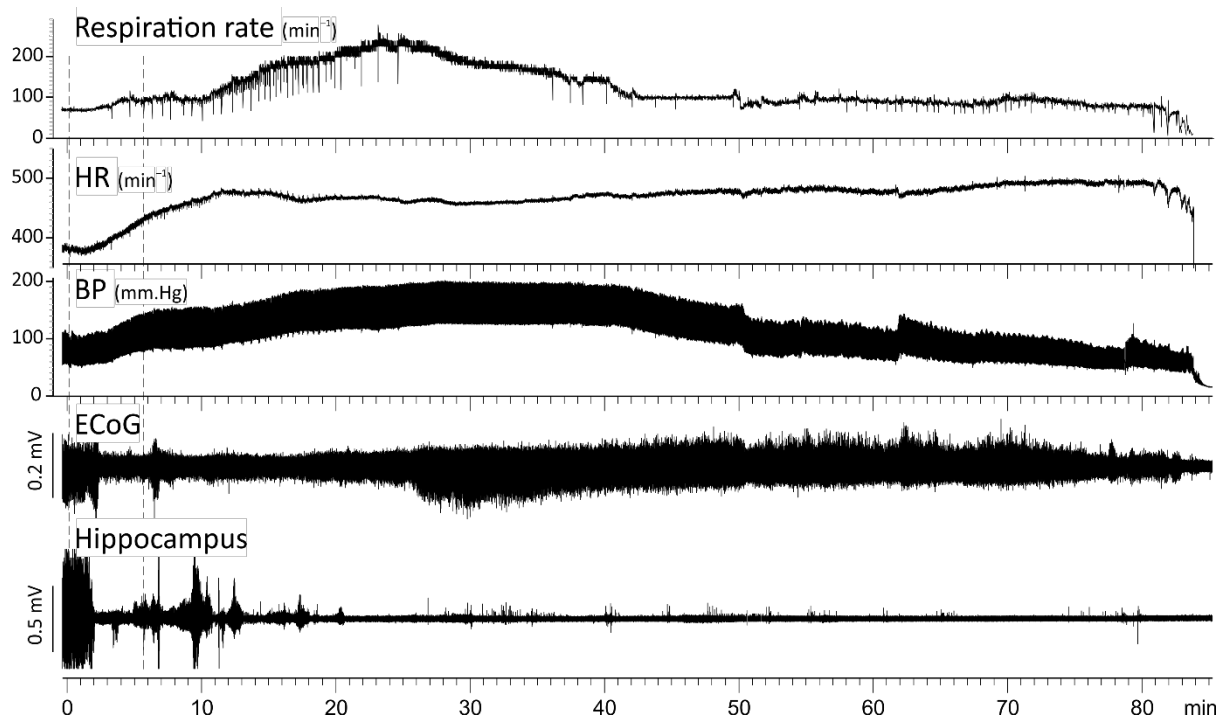


Figure 2. Central and cardiorespiratory consequences of intrahippocampal injection of kainic acid. Dashed lines mark the start and end of the 5-min injection. Respiration rate (top trace) more than doubles before dropping again; summary data are shown in the top box plot to the right (shows median, with 10th, 25th, 75th and 90th percentiles, with baseline measurement to left and peak value to right). Transients on respiration rate are due to augmented breaths (see Fig. 3), except for the final 3 minutes when transient apnoeas appear (see Fig. 4). Tachycardia (2nd trace) continues until death. Summary data are shown in the middle box plot to the right. Blood pressure (3rd trace) increases and then declines after approximately 40 min; summary data are shown in the bottom box plot to the right. ECoG and hippocampal field potentials show abolition of spontaneous oscillations related to urethane anaesthesia within the first 2 minutes of injection, with subsequent repeated episodes of electrographic seizures continuing until death. Time course varies considerably between rats, but broad features are very consistent.

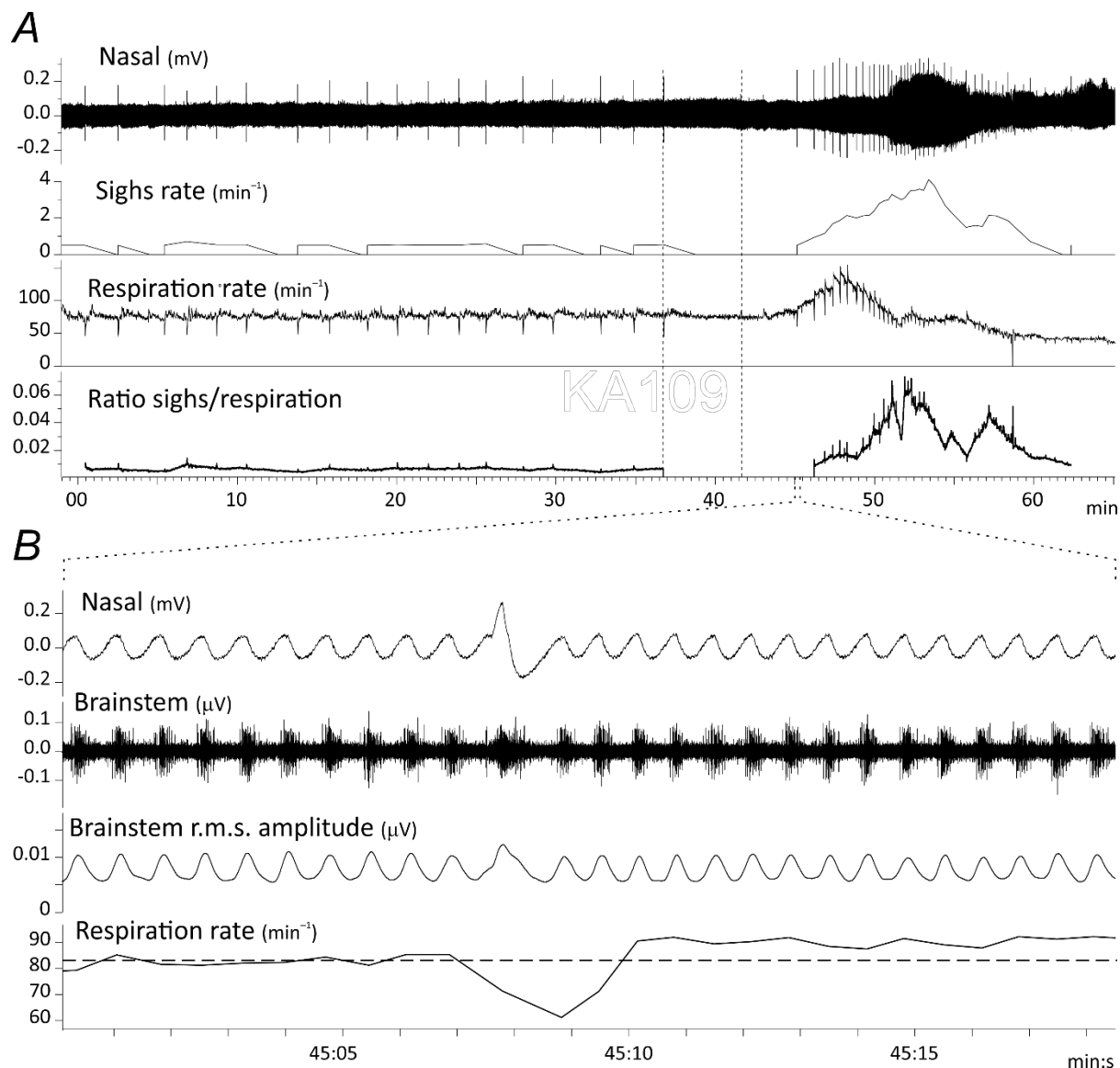


Figure 3. Augmented breaths, or sighs, are modulated by kainic acid injection. *A.* Respiration before and after injection of kainic acid (dashed vertical lines at 36.5 min) reveal sighs as transients (top trace), which disappear and then reappear at faster rate after 9.5 min. Below are plotted the rates of sighs and breaths (“respiration rate”) and their ratio, which reveals sighs increase as a proportion of breaths too. *B.* Expansion of segment of *A* at 45 min (marked by dashed lines between panels). A single sigh is shown amongst normal breaths (top trace). Respiratory brainstem neuron fires on the expiration (downward nasal signal), shown both as raw signal and root mean square amplitude. Note pause after sigh. Note, lag between respiratory neuron activity and nasal signal is due to neural and mechanical delays and thermal inertia in the thermocouple. Respiration rate (bottom trace) shows pause as decrease of rate, and also reveals acceleration of respiration for at least 8 minutes after the sigh.

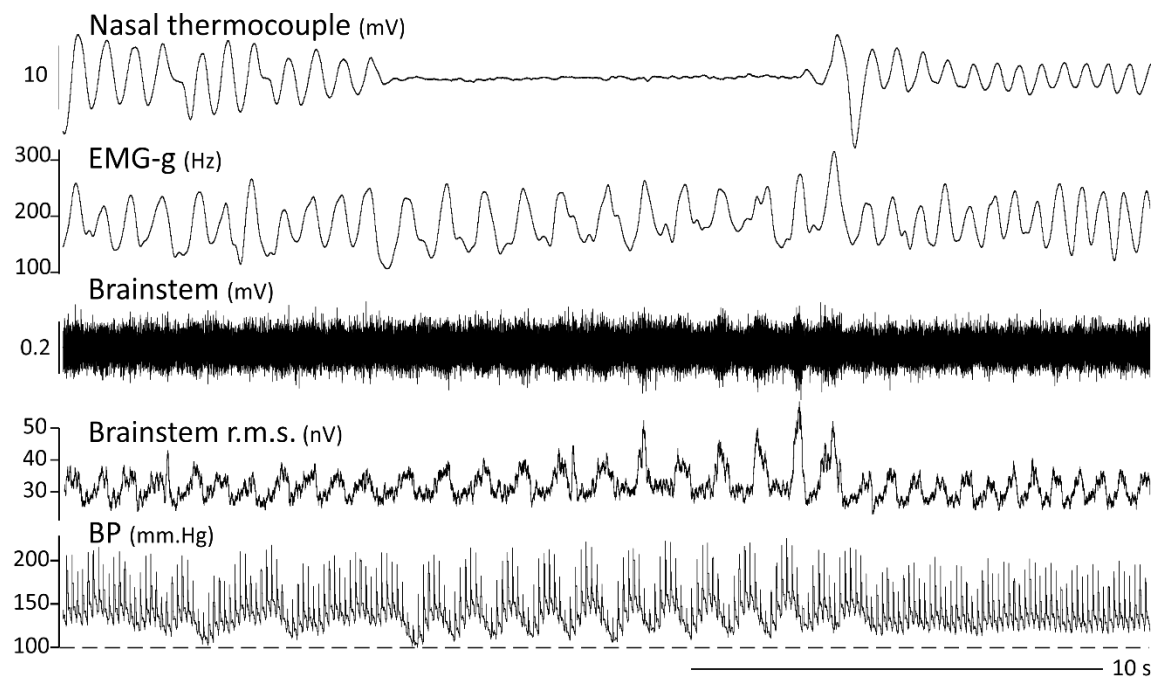
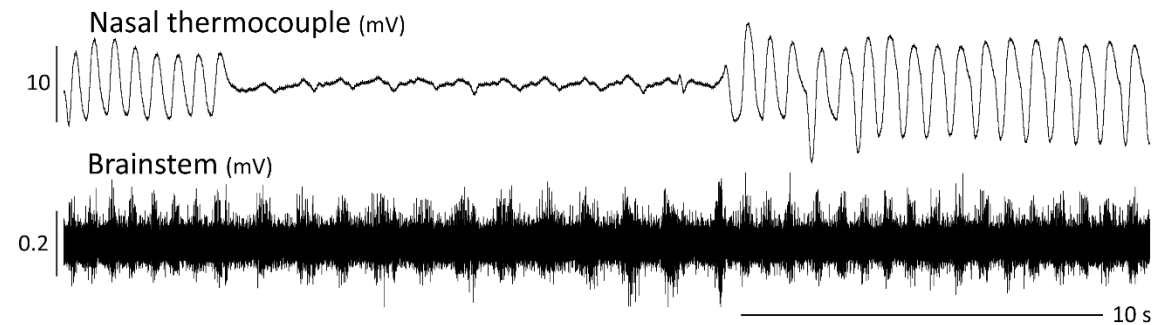
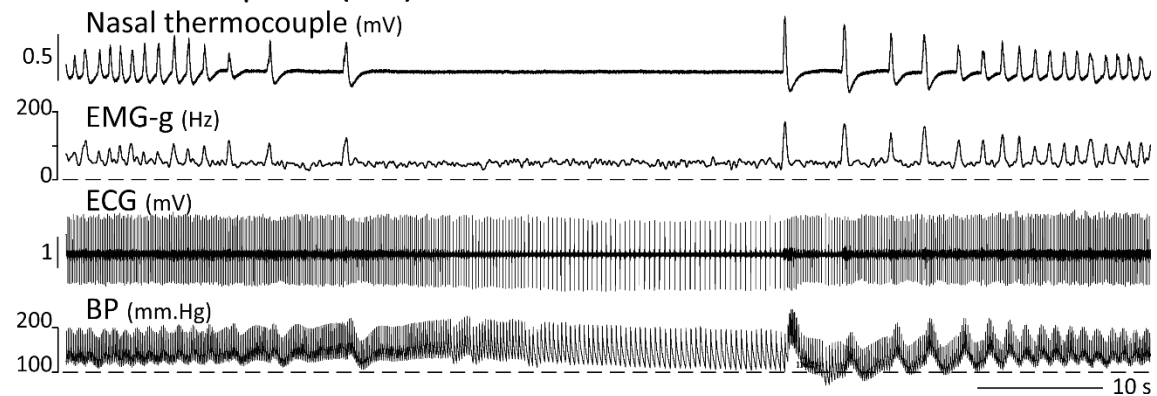
A Obstructive apnea (83%)**B Partial apnea (16%)****C Central apnea (1%)**

Figure 4. Transient apnoeas following intrahippocampal KA. **A.** Obstructive apnoeas are the most common. During apnoea (loss of oscillation of nasal thermocouple signal), extracted EMG (EMG-g) and brainstem firing continue at a lower rate. In this case brainstem activity is clearer on the r.m.s. measurement of the brainstem recording. Blood pressure shows oscillations in time with attempts to breath. **B.** Partial apnoeas have reduced amplitude nasal signals, indicating reduced airflow, but otherwise resemble obstructive apnoeas. In this case only the brainstem unit recording is shown. **C.** Central apnoeas are rare and show no evidence of respiratory effort on EMG-g and no modulation of blood pressure. Heartrate slows during central apnoea and blood pressure declines.

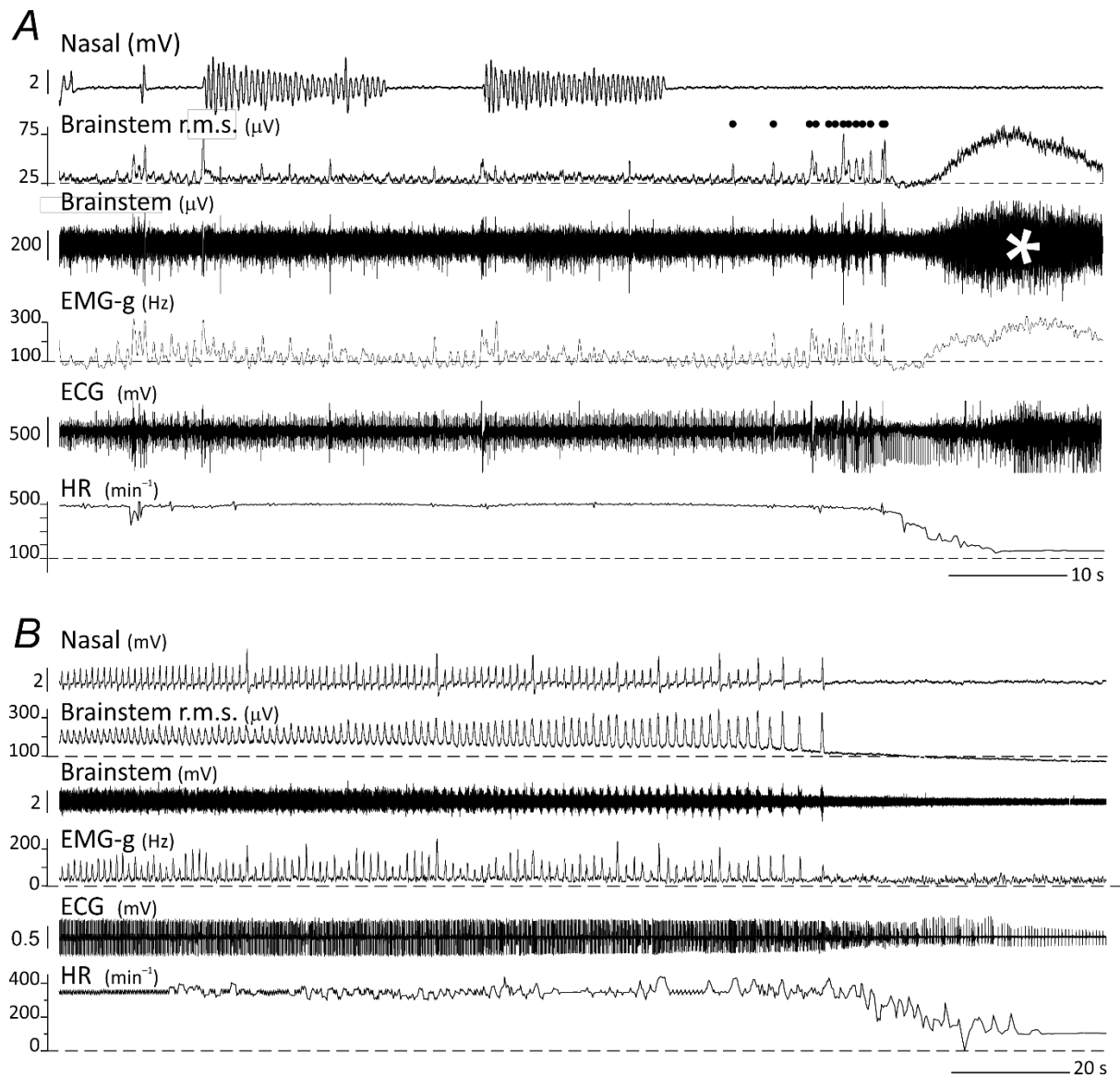


Figure 5. Lethal apnoeas following seizures induced by KA. **A.** Obstructive lethal apnoea. Nasal thermocouple reveals two transient apnoeas followed by the lethal terminal apnoea. Brainstem r.m.s. and raw recordings reveal increasing strength of activity with repeated attempts to breath (marked by filled circles over r.m.s. trace). Increased ineffective efforts to breath also appear as large amplitude derived EMG signals (EMG-g). Brainstem recording also reveals large discharge following the final attempt to breath (marked by white star). Heart rate slows after last attempt to breath. **B.** Central lethal apnoea. Same types of channel as in A, showing that all breaths apparent on the nasal recording are matched by brainstem activity and EMG-g. Respiration slows during final seconds. Heart rate again slows over several seconds after final breath.

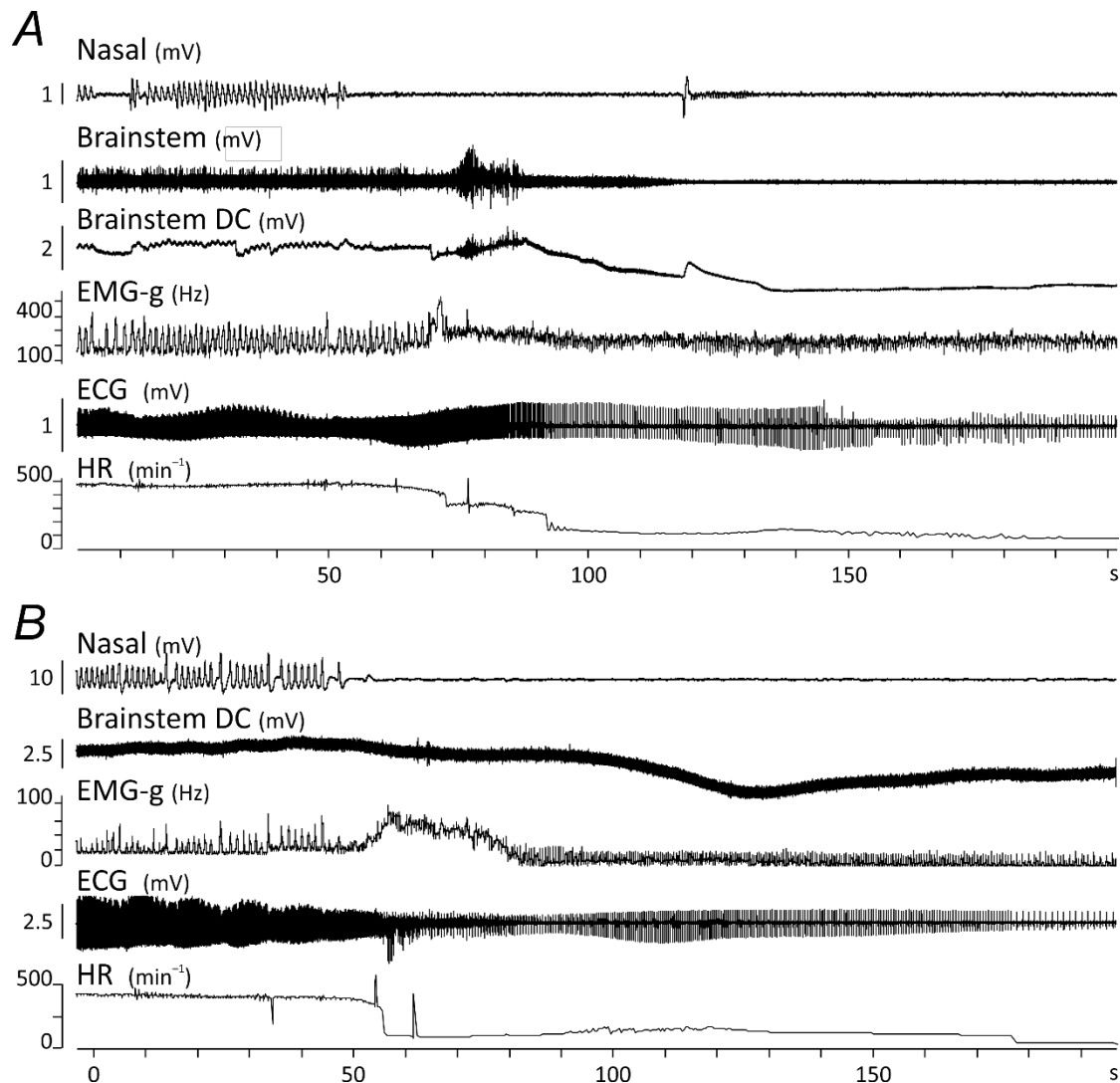
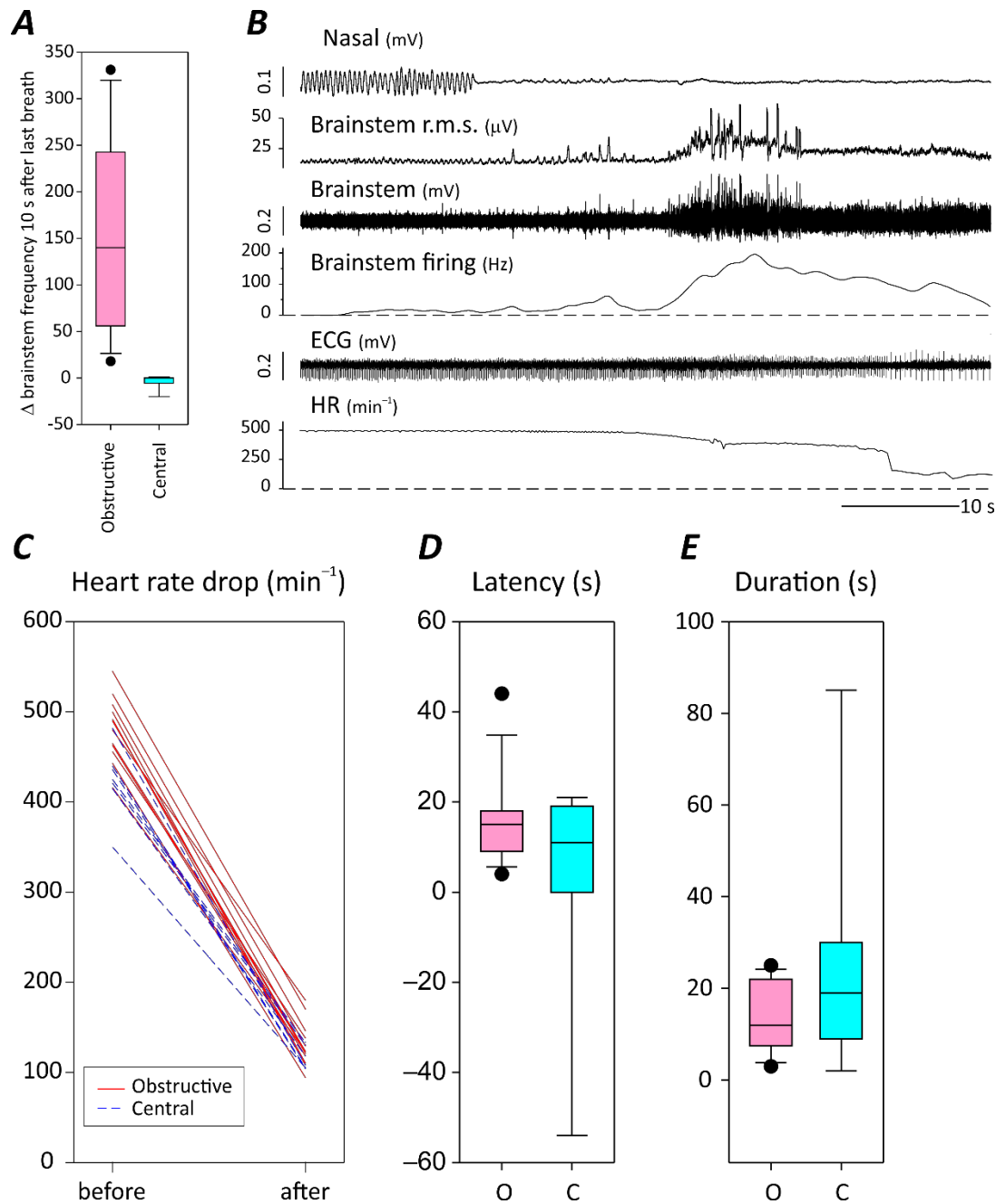
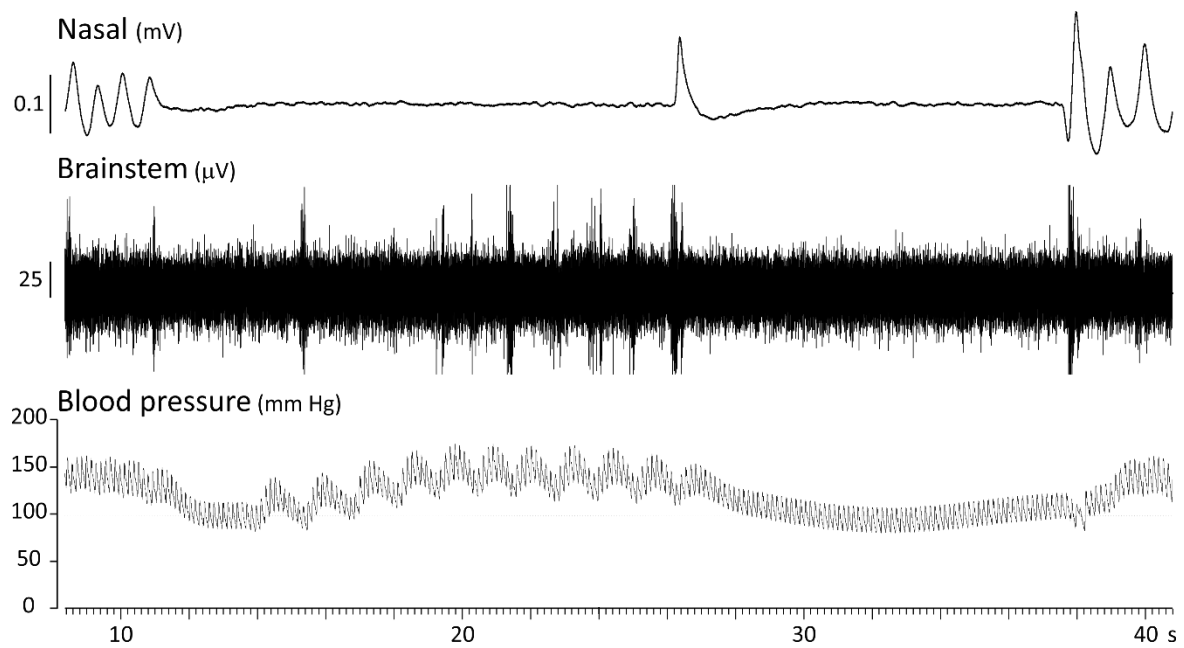


Figure 6. DC shifts recorded in 125- μ m conditioned silver brainstem electrode following lethal apnoeas. **A.** Obstructive lethal apnoea. As in Fig. 5 nasal signal shows cessation of respiration while brainstem unit activity (recorded with 25- μ m Pt/Ir electrode) and derived EMG activity continue for over 10 s. Note brainstem discharge on both brainstem recordings following final attempt to breath. DC brainstem recording (3rd trace) shows slow negative shift of voltage, in this case by -2 mV. Slowing of heartrate is clearly visible on the ECG as well as the heartrate traces. **B.** Central lethal apnoea. Following final breath (nasal signal), EMG evidence of efforts to breath cease. DC recording from brainstem shows slow negative shift after final breath, in this case to -1.6 mV. There is no evidence of a brainstem discharge following final breath. ECG and heartrate show slowing of heartrate after final breath, in this case faster than in panel A.



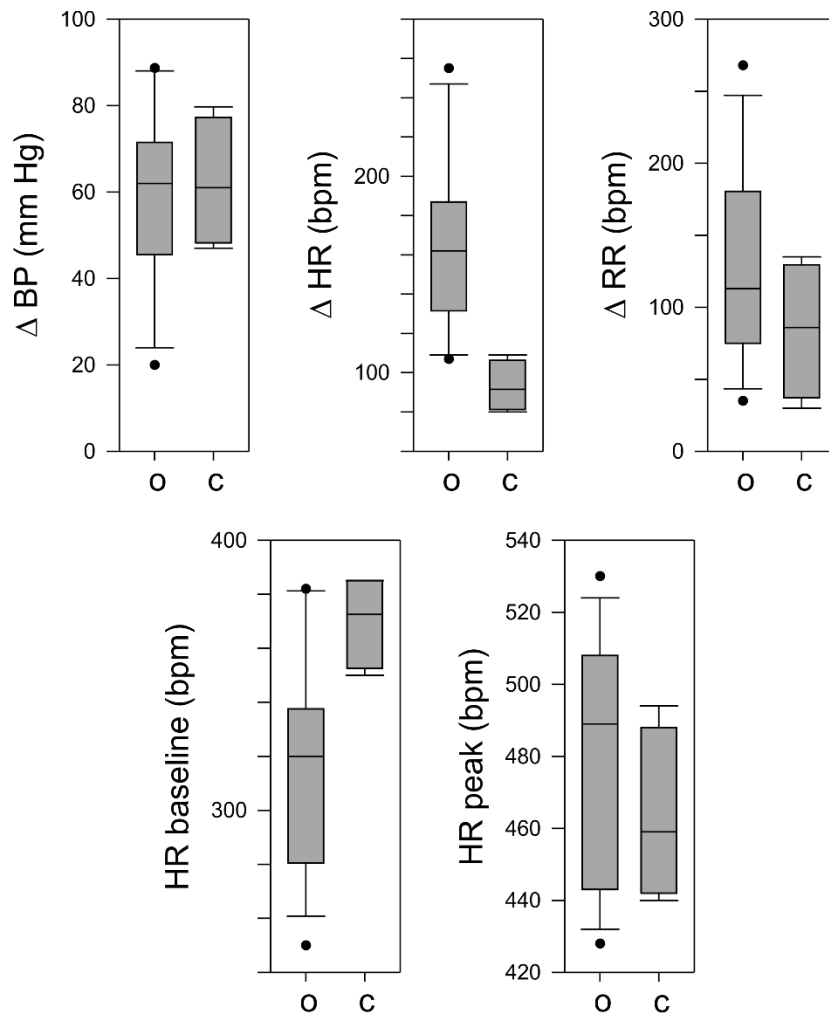
Supplemental Fig. S1

Brainstem discharge and heart rate collapse following final breath. **A**. Increased maximal brainstem firing rate 10–20 s after final breath or attempt to breath as a multiple of maximal firing rate during the previous 10 s (change: $p < 0.001$ Mann-Whitney U test). Firing rate is measured by rate of crossings of a threshold voltage. **B**. Obstructive fatal apnoea showing continued rhythmic activity of brainstem respiratory neurons after final breath, followed by large neuronal discharge (shown on r.m.s., raw signal and firing rate). ECG shows visible slowing, quantified in the heart rate trace below. The remainder of this figure concerns the most abrupt section of the heart rate drop, which is clearly visible in the raw ECG trace. **C**. The rapid drop in heart rate does not differ significantly between rats dying from obstructive (red lines) and central (dashed blue lines) apnoeas. Each line represents one rat ($p = 0.014$; HR before drop is significantly lower for central apnoeas, $p \leq 0.003$, but HR after is not, $p = 0.14$). **D**. Latency to onset of rapid HR drop does not differ between obstructive and central terminal apnoeas ($p = 0.18$, Mann-Whitney U test). **E**. Duration of rapid HR drop does not differ between obstructive and central apnoeas. Statistics are cited in the main text ($p = 0.70$, Mann-Whitney U test).



Supplemental Fig. S2

Sequential obstructive and central transient apnoeas. Prolonged (26-s) apnoea split by a single breath with a preceding obstructive apnoea lasting 15 s and a subsequent central apnoea lasting 10.5 s. Respiratory brainstem activity is visible during the obstructive apnoea but not during the central apnoea. Blood pressure oscillates with attempts to breath during obstructive apnoea, but declines smoothly during central apnoea, and also at the very start of the whole event.



Supplemental Fig. S3

Physiological changes preceding deaths by apnoea that are obstructive (boxes labelled “o”) and central (“c”). Seizure-related increases in BP (Δ BP) and respiration rate (Δ RR) did not differ between the two groups (t tests $P=0.32$ and 0.8 , respectively), but heartrate did (Δ HR; t-test $P<0.005$). All 3 physiological measures approach their maximal values during seizures, including heartrate, so maximal heartrate did not differ between the two groups ($P=0.12$) but the baseline heartrate preceding KA injection did ($P<0.04$). The relevance, and robustness, of this observation remains to be determined.